International Journal of Engineering Research and Technology. ISSN 0974-3154, Volume 12, Number 2 (2019), pp. 141-150

Numerical Investigation of Geometry Parameters for Axisymmetric Plug Nozzle Design at High Temperature

Ahmed Abdallah Elhirtsi[1], Toufik Zebbiche[2]

[1]*Aeronautical Sciences Laboratory, Institute of Aeronautics and Space Studies, University of Blida 1, BP 270 Blida 09000, Algeria.*

[2]*Aeronautical Sciences Laboratory, Institute of Aeronautics and Space Studies, University of Blida 1, BP 270 Blida 09000, Algeria.*

Abstract

The aim of this work is the design and numerical analysis of supersonic axisymmetric plug nozzle at high temperature of flow. The method used is based on the theory of Prandtl-Meyer expansion, using the characteristics method. A Fortran programming language has been realized. When the nozzle contour is obtained, the calculation of thermodynamic parameters (pressure, temperature, density and Mach number) are carried out. The error calculation is made between our model at high temperature of air flow and the perfect gas model. In terms of design parameters (length, thrust coefficient and mass coefficient), the performances obtained for the axisymmetric nozzle are clearly better than those obtained for bidimensionnel nozzle.

Keywords: Supersonic Nozzle Design, Prandtl Meyer Function, High Temperature, Method of Characteristics.

Nomenclature

A	Section Area (m^2)
C_F	Coefficient of the pressure force
C_{Gas}	Coefficient of the mass of the gas
C_{mass}	Coefficient of the mass of the structure
C_P	Specific heat to constant pressure
C^+	Right running characteristic
C^-	Left running characteristic
Fx	Axial pressure force exerted on the wall
EDN	Abreviation of the word Expansion Deflexion Nozzle
H	Enthalpy except for a constant
HT	Abreviation of the word *High Temperature*
L	Length of the plug nozzle
M	Mach number
MOC	Abbreviation of method of Characteristics
Nc	Number of the discretization points
P	Static pressure
PG	Abreviation of the word *Perfect Gas*
PN	Abreviation of the word Plug Nozzle
R	Universal constant of a perfect Gas
r	Radial component
T	Temperature
t_M	Thickness of the structural plug material
x, y	Cartesian components
X_{plug}	Distance between the exit section and the lip
θ	Flow angle deviation
Δx	Non-dimensional step
ν	Prandtl Meyer function
μ	Mach angle
ρ	Density
ε	Relative error computation
γ	Specific heats ratio
φ	Polar angle of a Mach wave
ψ	Deviation of the Lip compared to the vertical
λ_B	Polar radius at point B
λ_i	Polar radius at point i
σ	Interpolation coefficient of the pressure

Subscripts

0	Stagnation condition
$*$	Critical condition
E	Exit section
i	Node
(i)	Segment

International Journal of Engineering Research and Technology. ISSN 0974-3154, Volume 12, Number 2 (2019), pp. 141-150

1. INTRODUCTION

An aerospace vehicle is accelerated by a propulsion system at a speed imposed by specific requirements to the vehicle's mission. The nozzle is one of the most important components of this engine because its efficiency greatly affects the performance of the engine [1]. Unlike conventional bell-shaped nozzles, which operate optimally at a particular altitude, plug nozzles (Aerospike) allow the flow expansion to self-adjust, thus improving thrust coefficients. This improvement over conventional bell-shaped nozzles occurs at altitudes lower than the design altitude. At altitudes higher than the design altitude, plug nozzles essentially operate similarly to bell nozzles. The plug nozzle rocket engine has been selected for the space shuttle propulsion. A lot of investigation on aerospike nozzle has been carried by researchers. The activities concerned include contour design and its performance [2-6] and numerical simulations [7-9]. All this research has been developed for the case of a perfect gas model. This study assumes that the specific heat *Cp* is a constant value and does not vary with the temperature. It gives good results only if the two parameters M_E and T_0 are small, which do not exceed respectively about 2.00 and 240 K. If M_E begins to gradually exceed 2.00 to the supersonic limit taken (M_E = 5.00) or when T_0 begins to exceed 240 K up to the limit of 3550 K (since the application is for air), which is the case for the majority of aerospace applications. The results presented in these references are quite far from reality, since the physical behaviour of gas changes, and it becomes calorically imperfect and thermally perfect. In this case, the specific heat *Cp* becomes a function of temperature and the energy conservation equation changes completely. This model is called as model at High Temperature (*HT*), lower than the threshold of the molecules dissociation. The new model presented essentially depends on the stagnation temperature, which becomes an important parameter, in addition to the parameters of the perfect gas model [10-13]. In ref [14], the authors designed the contour and studies of the flow fields in the bi-dimensional plug nozzle for the model *HT*.

The aim of this work is, in the first step, to determine a new form of the supersonic axisymmetric Plug Nozzle (*PN*) and Expansion Deflexion Nozzle (*EDN*) giving a uniform and parallel flow at the exit section at high temperature. This study is to make corrections to the results using Perfect Gas model [15,16]. The second step of this study is to determine the parameters (θ^*, L/λ_A, A_E/A^*, P/P_0, T/T_0 and ρ/ρ_0)) in the flow fields points for the axisymmetric plug nozzle.

2. MATHEMATICAL FORMULATION

The difference between the plug nozzle and the other nozzle types, in particular the minimum length nozzle [19], is that the flow at the throat is inclined at an angle θ^* compared to the horizontal as illustrated in Fig. 1, which is not the case for other models where the flow at the throat is horizontal.

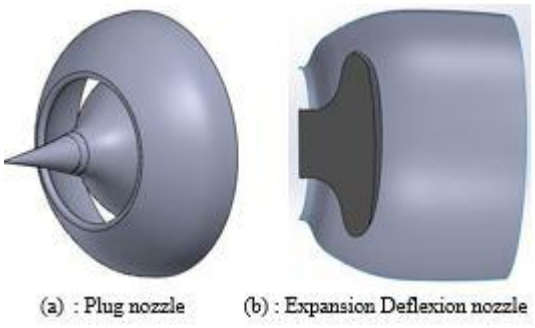

Fig. 1. Different configuration of plug nozzles

The lip of the central body must be inclined at an angle ψ compared to the vertical. As the deviation of the flow at the throat is not zero, the flow through the central body straighten from the angle $\theta=\theta^*$ at the throat to the angle $\theta=0$ at the exit. So, the nozzle shape must accelerate the flow from the Mach number $M=1$ at the throat to the exit section. This shape gives a uniform and parallel flow at the exit section of the nozzle [17]. The expansion of the axisymmetric plug nozzle does not generate a Kernel zone, but only a transition region *ABE* which represents a non-simple wave region which the solution is obtained numerically [17,18]. On the other hand, the region *AES* is a uniform flow zone with an exit Mach number M_E (see Fig. 2).

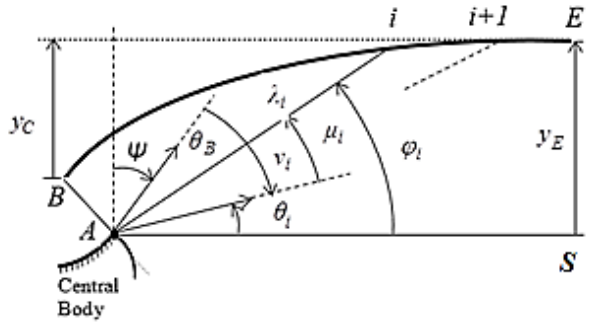

Fig. 2. Geometry relationship between Mach lines and flow direction

The flow calculation and the determination of the contour of the *HT* central body are based on the Prandtl-Meyer expansion [10-14] by:

$$\theta_E = \nu_E = \int_{T_E}^{T_*} F_\nu(T)\,\mathrm{d}T \qquad (1)$$

With:

$$F_\nu(T) = -\frac{C_P(T)}{2\,H(T)}\sqrt{\frac{2\,H(T)}{a^2(T)}-1} \qquad (2)$$

$$a(T) = \sqrt{\gamma(T)\,R\,T} \quad ; \quad M(T) = \sqrt{2\,\mathrm{H(T)}} \qquad (3)$$

The inclination of the lip compared to the vertical is determined by the relation (4). [14,17]

$$\psi = 90 - \nu_E \tag{4}$$

2.1 Discretization

The contour of the axisymmetric plug nozzle is determined at the same time as the calculation of the flow at the points of intersection of the characteristics in the transition region *ABE*. The properties of the points of the control surface *AE* are known and equal to the values of the uniform flow of the exit section M_E. The control of the geometry of the mesh in the transition region depends on the distance Δx chosen for the selected points on the uniform Mach line *AE*. Fig. 3 shows the process and direction of calculation in the transition region.

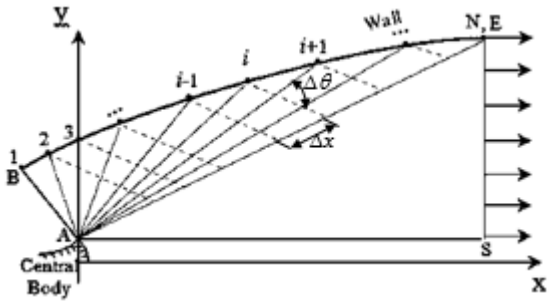

Fig. 3. Process of the discretization of the Plug and Expansion Deflexion Nozzles

The properties at points *A* and *B* are given by the following system:

$$\begin{cases} x_A = 0 \\ r_A = 0 \\ \theta_i = (i-1)\cdot\dfrac{\theta^*}{N} \\ \nu_i = \theta^* - \theta_i \\ M_i = f(\nu_i) \\ \mu_i = \sin^{-1}\left(\dfrac{1}{M_i}\right) \\ \text{avec: } i = 1 \text{ à } (n+1) \end{cases} ; \quad \begin{cases} x_B = x_A - r_c \cdot \sin(\phi) \\ r_B = r_A + r_c \cdot \cos(\phi) \\ \theta_B = \theta^* \\ \nu_B = 0 \\ M_B = 1 \\ \mu_B = \dfrac{\pi}{2} \end{cases} \tag{5}$$

PointA PointB

2.2 Calculation procedure

As C^- and C^+ are curved, the application of the *MOC* requires us to introduce a fine grid, in order to approximate each characteristic between two points by straight segments. Since a point in the supersonic flow field is related to two characteristics, one rising $C^+_{(1)}$ and the other descending $C^-_{(2)}$, the properties of the next point (*3*) can be obtained. The point (2) of the control surface *AE* is determined by the properties given by the system (6).

$$\begin{cases} x_2 = x_A + \Delta x \cdot \cos(\mu_E) \\ y_2 = r_A + \Delta x \cdot \sin(\mu_E) \\ \theta_2 = 0 \\ \nu_2 = \nu_E \\ M_2 = M_E \\ \mu_E = \sin^{-1}\left(\dfrac{1}{M_2}\right) \end{cases} \tag{6}$$

The first step is to calculate the first characteristic C^- and determine its corresponding point on the wall of the nozzle as shown in Fig. 4.

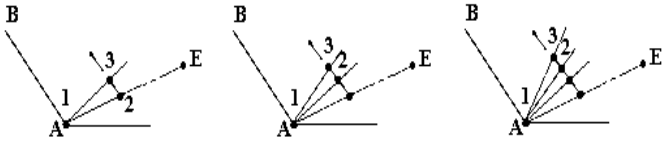

Fig. 4. Calculation process of C^-

The iterative method is based on the mean of the position and the properties of the point (3) as well as the position and the original properties of the characteristics $C^-_{(2)}$ and $C^+_{(1)}$. They will be used each time as starting conditions of their respective characteristics. This process is repeated until the convergence criteria of the flow direction is satisfied (see Fig. 5).

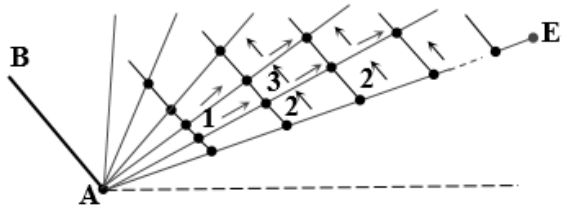

Fig. 5. Determination of the different characteristics C^- and C^+

For the axisymmetric supersonic, non-rotational, adiabatic flow of a perfect gas, the *MOC* gives the following equations known by characteristics and compatibilities equations [10,11,17,19]:

- Along C^-:

$$\begin{cases} d(\theta + \nu) = \dfrac{\sin\theta \sin\mu}{y \cos(\theta - \mu)} dx \\ \dfrac{dy}{dx} = \tan(\theta - \mu) \end{cases} \tag{7}$$

- Along C^+:

$$\begin{cases} d(\nu-\theta)=\dfrac{\sin\theta\sin\mu}{y\sin(\theta+\mu)}dy \\ \dfrac{dy}{dx}=\tan(\theta+\mu) \end{cases} \quad (8)$$

As the function *H(T)* depends on the parameter T_0 [10,11,19,20], the *HT* model depends primarily on the stagnation temperature T_0 of the combustion chamber.

After transformation of the relations (7) and (8), we obtains the following mathematical *HT* model of *MOC* [20]:

- Along C^-:

$$\begin{cases} \displaystyle\int_{T_{i-1}}^{T_{i+1}}\left[-\frac{Cp(T)}{2H(T)}\sqrt{M^2(T)-1}\right]dT+\int_{\theta_{i-1}}^{\theta_{i+1}}d\theta=\int_{x_{i-1}}^{x_{i+1}}\frac{\sin\theta\sin\mu}{y\cos(\theta-\mu)}dx \\ \displaystyle\int_{T_{i-1}}^{T_{i+1}}dy=\int_{x_{i-1}}^{x_{i+1}}\tan(\theta-\mu)dx \end{cases} \quad (9)$$

- Along C^+:

$$\begin{cases} \displaystyle\int_{T_i}^{T_{i+1}}\left[-\frac{Cp(T)}{2H(T)}\sqrt{M^2(T)-1}\right]dT+\int_{\theta_i}^{\theta_{i+1}}d\theta=\int_{x_i}^{x_{i+1}}\frac{\sin\theta\sin\mu}{y\sin(\theta+\mu)}dx \\ \displaystyle\int_{T_i}^{T_{i+1}}dy=\int_{x_i}^{x_{i+1}}\tan(\theta+\mu)dx \end{cases} \quad (10)$$

To evaluate the integrals in relations (9) and (10), it is necessary to make appropriate approximations so that the physical phenomenon and the mathematical considerations in the interval considered.

Equations of characteristics and compatibilities are ordinary non-linear equations. Their solution will be sought by the application of the finite difference technique [18]. The mesh established assume the portion of the characteristic between two points by straight line segments. The numerical integration method employed is that of Euler which is of the predictor-corrector type [10-13,20]. The Euler corrector algorithm iterations is repeated until reaching the desired accuracy ε.

3. ERROR ASSOCIATED WITH THE PERFECT GAS MODEL

A comparison between the results given by the two models will be made. For each value of the stagnation temperature T_0 and the exit Mach number M_E, the relative error can be evaluated for the *PG* model compared with the *HT* model for each design parameter by the following relation:

$$\varepsilon_{(Parameter)}\% = \left|\frac{(Parameter)_{HT}-(Parameter)_{PG}}{(Parameter)_{HT}}\right|\times 100 \quad (11)$$

Where $(Parameter)_{PG}$ and $(Parameter)_{HT}$ represent the values of calculated parameters by using *PG* and *HT* model respectively.

4. RESULTS AND COMMENTS

The design results of the axisymmetric plug nozzle are presented in non-dimensional form for three values of the stagnation temperatures T_0=1000 K, T_0=2000 K and T_0=3000 K. The perfect gas case is illustrated for each parameter, in particular, one application is made for air. In this case, the specific heat function C_p and the universal gas constant of the perfect gas *R* for air case are used.

4.1. Grid in the characteristics

Figs. 6–7 present the grids in the characteristics by exploitation of the various parameters intervening on the grid generation. Each parameter has an importance which influences the results of design. The nature of a supersonic flow depends on the upstream condition. An error at the beginning of calculation (throat) propagated, in order to be rather large at the exit section. In addition, the errors caused by calculating mathematical operations called artificial viscosity. The selected example is for T_0 = 2000 K and M_E = 3.00.

In Fig. 6, when we refine the grid in the expansion zone between the Mach waves of the throat and the exit section, we can discretize this zone into *N* Mach waves (*Nc*). Three examples are presented on the cases (a), (b) and (c), when inserting respectively, *Nc*=10, *Nc*=30 and *Nc*=50. It is noticed that more the Mach waves number *Nc* is large, we obtain a very good presentation of the central body. Then the refinement in this area can decrease the error.

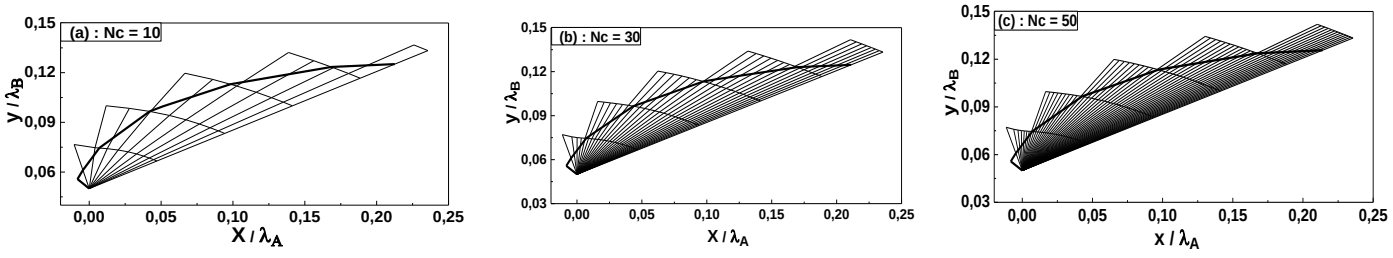

Fig. 6. Grid refinement of Mach wave (*Nc*) on the design of axisymmetric plug nozzle

Fig. 7 presents some grids with insertion of additional step Δx for Nc=50. It is clear that a higher number of points Nc gives a very good presentation for the contour of the plug nozzle. The control of the results is done by the use of the ratio of the sections which remains always valid since the flow at the exit of the nozzle is uniform and parallel. It should be noted that there are design parameters dependent on the pitch Δx and the number of characteristics Nc.

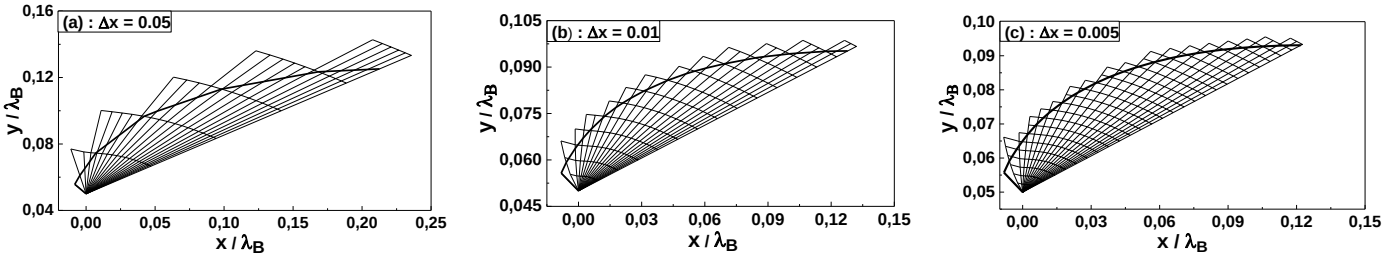

Fig. 7. Grid refinement of step Δx on the design of axisymmetric plug nozzle.

Figs 8-11 illustrate the contours of the flow fields obtained numerically by our calculation code, the different design parameters (iso-Mach, pressure ratios P/P_0, temperature ratios T/T_0 and densities ρ/ρ_0) of the axisymmetric plug nozzle.

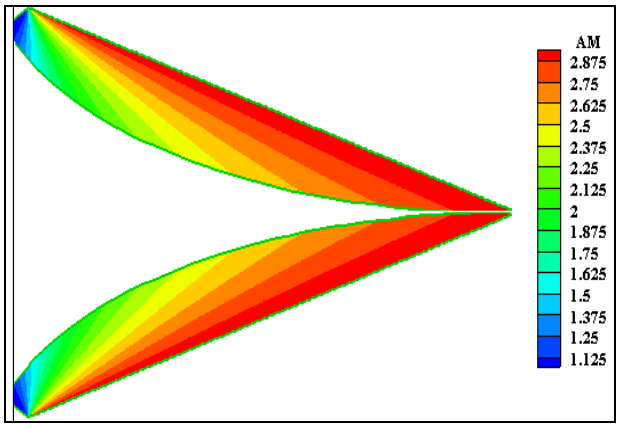

Fig. 8. Iso-Mach of the axisymmetric plug nozzle

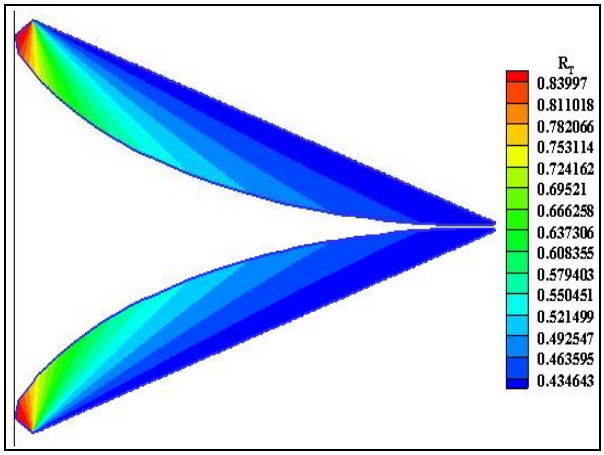

Fig.9. Iso-Temperatures ratio (T/T_0) curves

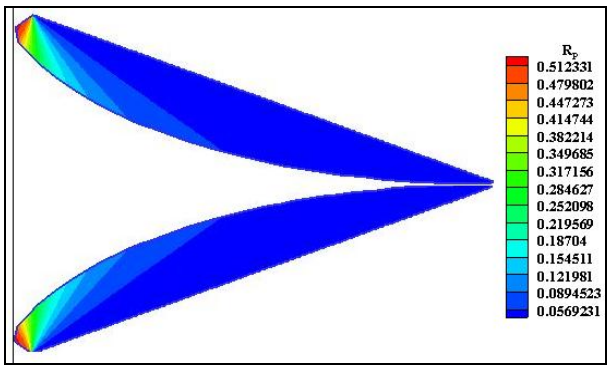

Fig.10. Iso-Pression ratio (P/P_0) curves

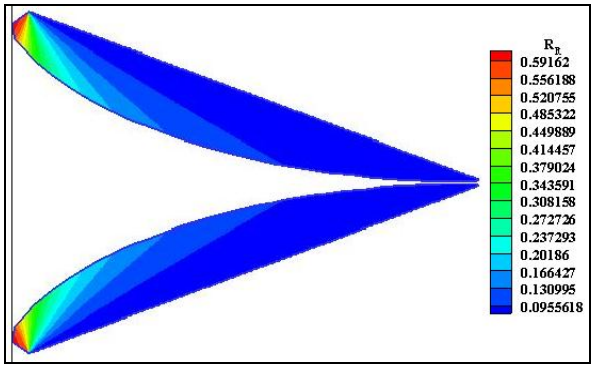

Fig.11. Iso-Density ratio (ρ/ρ_0) curves

4.2. Effect of T_0 on the plug contour

Figs. 12 (a-d) illustrate the influence of the stagnation temperature T_0 on the design of the contour of the axisymmetric central body nozzle as a function of the exit Mach number of the nozzle. Indeed, the calculations were carried out for three different values of T_0, by varying the exit Mach number M_E from 2.00 to 5.00. In these figures, it has been found that by increasing the exit Mach number, the evolution of the stagnation temperature has a considerable influence on the nozzle contour. In Figure 12 (a), for an exit Mach number equal to 2.00, it is noted that the three curves

obtained for the three values of the stagnation temperature T_0 are almost identical with that obtained for the case of a perfect gas. On the other hand, for the curves obtained at exit Mach numbers greater than 2.00, the difference becomes larger and increases as a function of the temperature T_0 and as a function of the exit Mach number M_E.

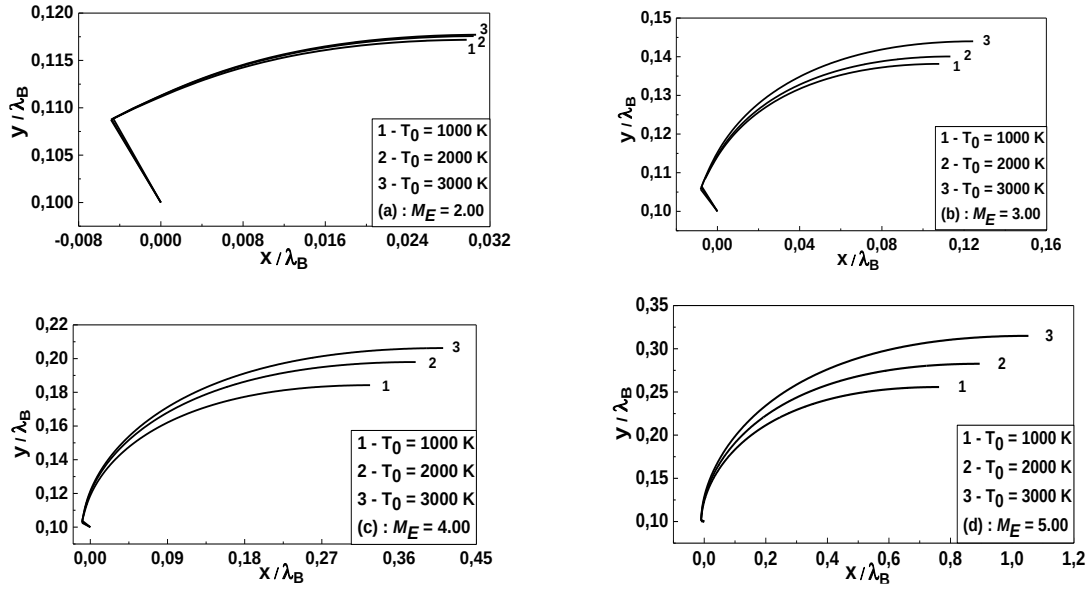

Fig.12. Effect of the stagnation temperature T_0 on the axisymmetric Plug Nozzle and external *EDN* wall shape giving different exit Mach number M_E

Table 1 shows the effect of the stagnation temperature T_0 on the design of the axisymmetric central body nozzle for a Mach number M_E = 5.00. Note that the thrust coefficient increases with the increase of T_0.

Table 1

Effect of the stagnation temperature T_0 on the axisymmetric Plug Nozzle design for M_E = 5.00

	θ^*	L/λ_A	As/A*	C_{Mass}	C_F
PG	76.714	73.580	25.510	164.199	1.407
T_0=1000 K	78.983	77.253	27.426	177.575	1.478
T_0=2000 K	84.263	90.453	24.759	229.017	1.633
T_0=3000 K	87.617	105.702	44.120	295.115	1.791

4.3. Variation of Design Parameters according to M_E

Fig. 13 represents the variation of the angle θ* just after the throat of the axisymmetric plug nozzle as a function of the exit Mach number M_E. Note that, the higher the nozzle delivers a high exit Mach number M_E, the angle of deflection becomes larger (the nozzle becomes more open to the throat) to allow an appropriate expansion adapted, therefore, to give a uniform flow and parallel to the exit. Similarly, for an exit Mach number M_E given, the higher stagnation temperature T_0 increases, the angle of deviation of the throat of the nozzle becomes larger.

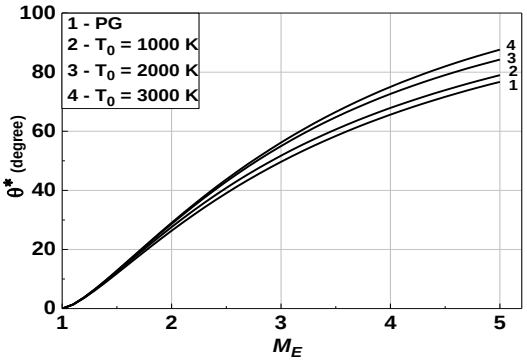

Fig.13. Variation of θ^* versus M_E

Fig. 14 shows the variation of the axisymmetric central body nozzle length as a function of the exit Mach number M_E for different values of the stagnation temperature T_0. Note that the length of the nozzle increases not only with the increase of M_E, but also with the increase of T_0.

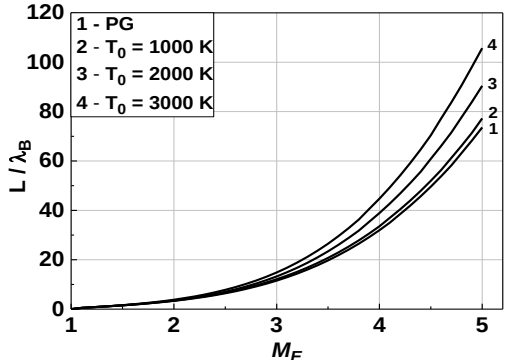

Fig.14. Variation of L/y^* versus M_E

Fig. 15 shows the variation of the section ratio (A_E/A^*) as a function of the exit Mach number M_E. Note the evolution of (A_E/A^*) is the same as that of the length of the axisymmetric plug nozzle.

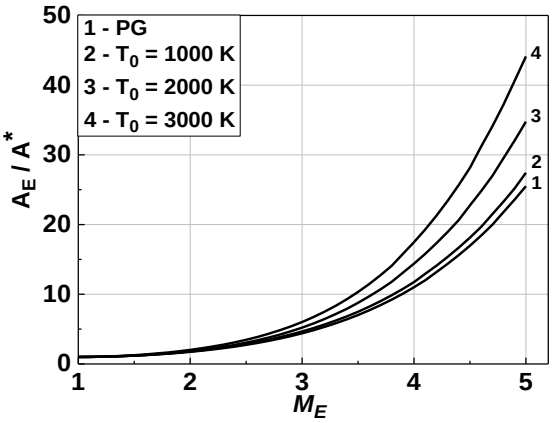

Fig.15. Variation of section ratio versus M_E

Fig. 16 represents the variation of the coefficient of the mass of the axisymmetric central body nozzle as a function of the exit Mach number M_E for different values of the stagnation temperature T_0. It should be noted that the difference between the curve *PG* and the other curves obtained for the different temperatures T_0 is negligible for an exit number Mach less than 2.00. This difference becomes greater and increases more when the exit Mach number M_E increases. It is concluded that more the nozzle delivers a high exit Mach number M_E, the larger the mass becomes. For low values of M_E and T_0, the four curves fuses and start to be differs when M_E>2.00. The curves corresponding at *PG* and T_0=1000 K are almost superposed for any value of M_E. This result shows that the *PG* model can be used for T_0<1000 K.

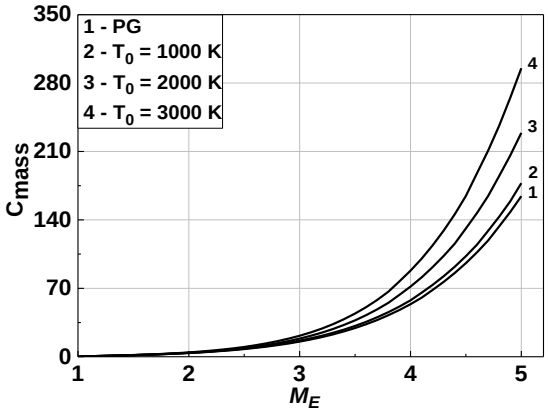

Fig.16. Variation of C_{Mass} versus M_E

Fig. 17 shows the variation of the thrust coefficient exerted on the axisymmetric central body nozzle profile as a function of the exit Mach number M_E for different values of the stagnation temperature T_0. It should be noted that the influence of the stagnation temperature T_0 on the thrust coefficient C_F is negligible when the exit Mach number M_E is less than 1.50, but beyond this value, the difference between the three curves of the *HT* model increases gradually with the increase of M_E.

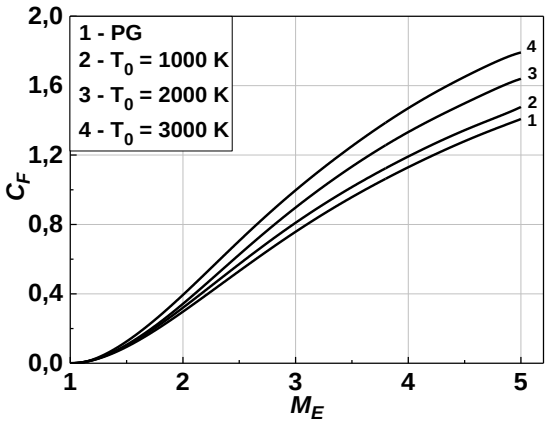

Fig.17. Variation of C_F versus M_E

4.4. Variation of Thermodynamic Parameters along the Wall of the Central Body

Fig. 18 shows the evolution of the T/T_0 ratio along the nozzle contour. This figure has been numerically produced by our calculation code for M_E=3.00 and T_0=2000 K. The T/T_0 parameter allows us to appropriately choose the constructive material that will withstand this temperature. It is maximal at the level of the throat and then decreases along the contour of the nozzle for all gases. For example, if T_0=2000 K, then value of the temperature at the throat is T^*=1665.28 K and T_E=712 K at the exit of contour for the *PG* model. For the *HT* model the temperature is T^*=1737.84 K and T_E=811.38 K. Similarly the P/P_0 ratio, is used to determine the pressure force exerted on the divergent wall.

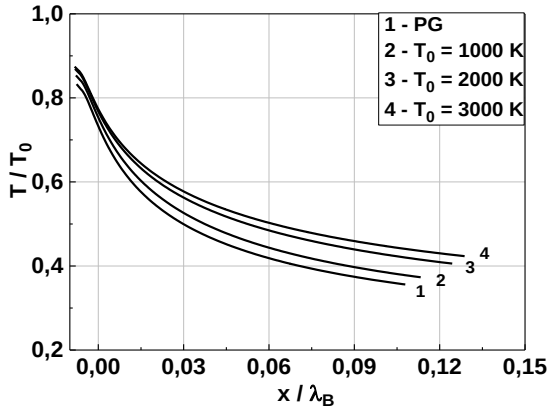

Fig.18. Variation of T/T_0 along the wall for M_E=3.00

Fig. 19 shows a pressure decay across the divergent part of the nozzle which will be transformed into thrust energy. This quantity is also used to study the distribution of radial and tangential stresses in order to study the resistance of the material. The ratio ρ/ρ_0 is an indicator for the quantity of the gas that which will pass through the divergent part in order to determine the fuel consumption (Fig. 20).

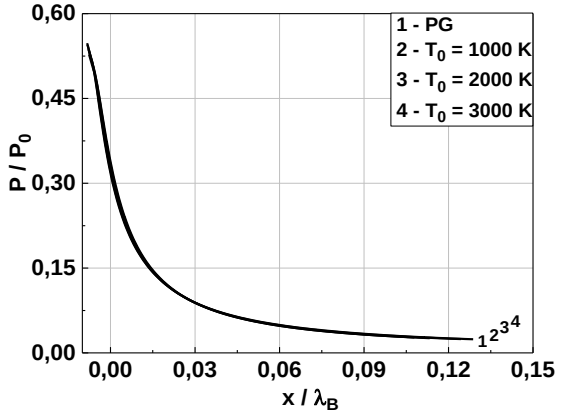

Fig.19. Variation of P/P_0 along the wall for M_E=3.00

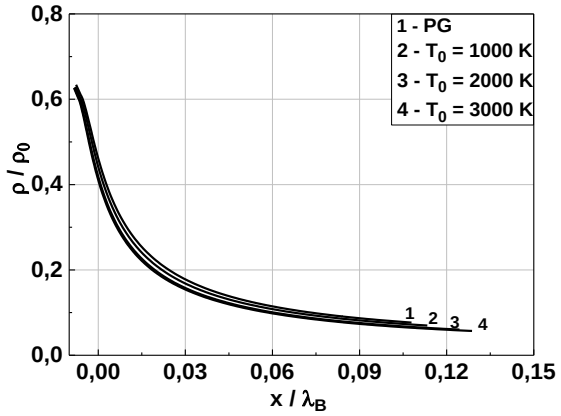

Fig.20. Variation of ρ/ρ_0 along the wall M_E=3.00

Fig. 21 shows the variation of the Mach number M along the wall of the axisymmetric plug nozzle for different values of the stagnation temperature T_0 and for an exit Mach number M_E=3.00. The increase in the Mach number is due to the expansion of the gas.

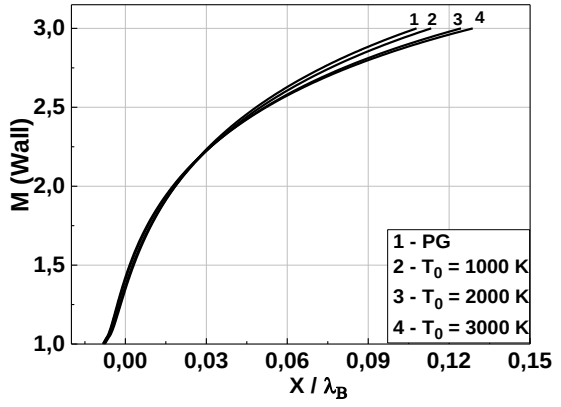

Fig.21. Variation of M along the wall for M_E = 3.00

Fig. 22 shows the variation of the flow angle deviation along the wall of the nozzle. One notices the existence of a deflection point closer to the throat. The flow expansion varies from $\theta=\theta_d=\theta^*$ at the nozzle throat (M=1), then increases to $\theta=\theta_{max}$ at the point of deflection and decreases to θ=0 in exit section, because the flow is uniform and parallel. In this case, we will have increase the efficiency of the nozzle and decrease the losses

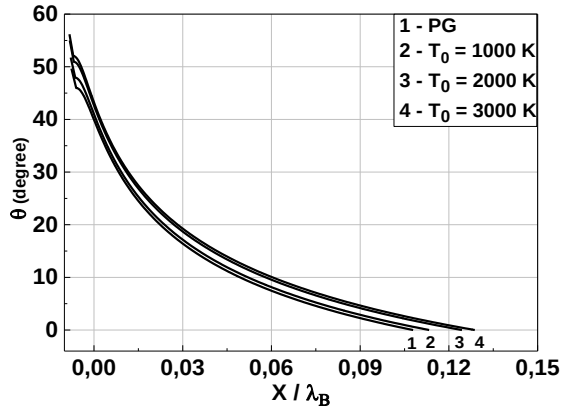

Fig.22. Variation of θ along the wall for M_E=3.00

4.5. Error caused by the Perfect Gas model

The perfect model (*PG)* is developed on the basis of considering the specific heat C_p constant, which gives acceptable results for low T_0 and M_E. According to this study, a difference in the results given between the *PG* model and our *HT* model will be presented. The error given by the *PG* model with respect to our *HT* model can be calculated for each parameter. Fig.23-25 give the variation of the relative error versus M_E for the length (L/λ_A), mass coefficient (C_{mass}) and thrust coefficient (C_F). For example, if T_0=2000 K and M_E=3.00, the use of the *PG* model will give a relative error equal to ε=12.825 % for the length, ε=16.547 % for mass coefficient and ε=15.641 % for the thrust coefficient. For lower values of M_E and T_0, the error ε is weak (less than 5%), which is interpreted by the use of the *PG* model when $T0$<1000 K or M_E<2.00.

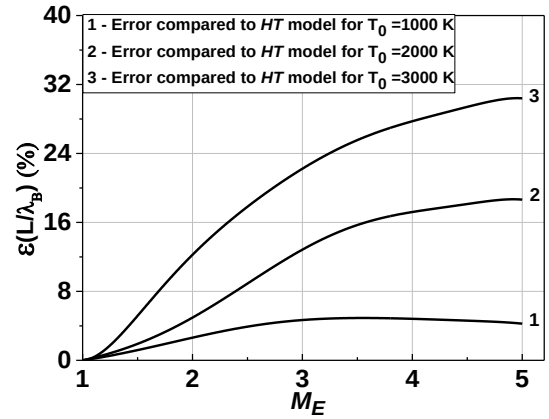

Fig.23. Variation of the relative error given by the length of the *PG* model versus M_E

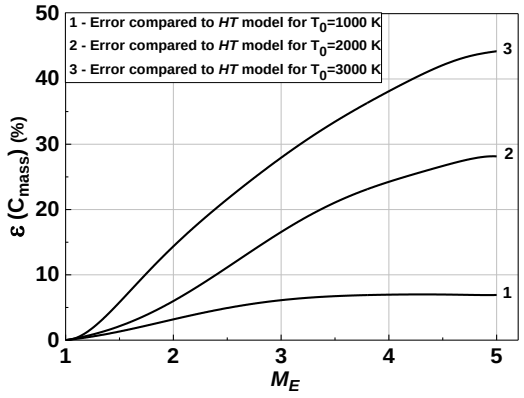

Fig.24. Variation of the relative error given by the Mass coefficient of the *PG* model versus M_E

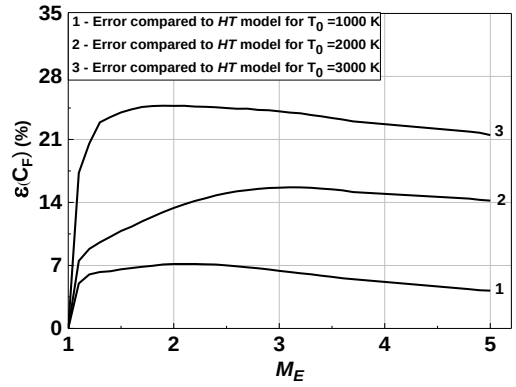

Fig.25. Variation of the relative error given by the thrust coefficient of the *PG* model versus M_E

4.6. Comparison to the 2D and axisymmetric plug nozzles

Fig. 26 represents the comparison between the lengths of bi-dimensional and axisymmetric plug nozzles for T_0=2000 K versus of the exit Mach number M_E. It can be noted that the curves of each figure representing the numerical results of each nozzle type are almost identical up to *ME*=3.00. But, beyond this value, they begin to be different as *ME* increases. For example, if M_E=5.00, the error obtained is 45.358 %.

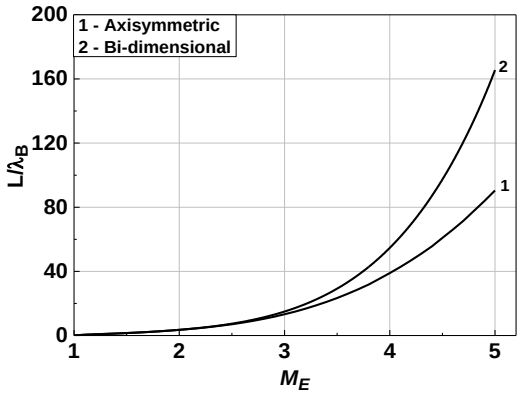

Fig.26. Comparison between the lengths of axisymmetric and bi-dimensional plug nozzles.

Fig. 27 shows the comparison between the thrust coefficient of bi-dimensional and axisymmetric plug nozzles for T_0=2000 K versus of the exit Mach number M_E. It is clearly noticed that the thrust coefficient for two plug nozzle types are almost confounded for any value of the exit Mach number M_E with an error not exceeding 0.54048 %.

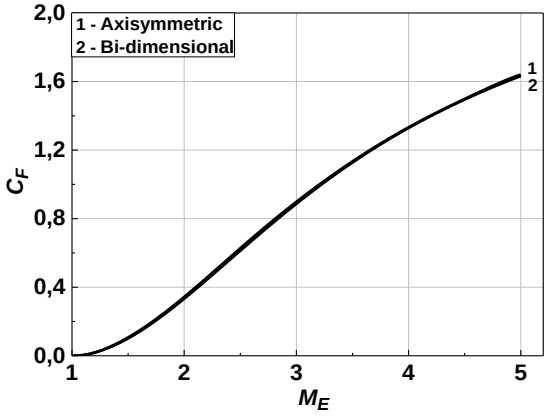

Fig.27. Comparison between the thrust coefficients of axisymmetric and bi-dimensional plug nozzles.

Fig. 28 shows the comparison between the mass coefficient of bi-dimensional and axisymmetric plug nozzles for T_0=2000 K versus of the exit Mach number M_E. More M_E increases, More the difference between the two nozzles types increases, and becomes considerable starting from M_E > 2.00. For example, the error is 34.0431 % when M_E=5.00.

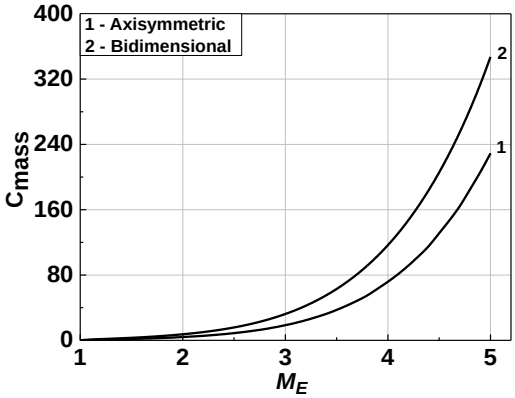

Fig.28. Comparison between the mass coefficient of axisymmetric and bi-dimensional plug nozzles.

5. CONCLUSION

This work allowed us to study the effect of the stagnation temperature T_0 on the design parameters of the supersonic axisymmetric plug nozzle using the characteristics method at high temperature. A Fortran language calculation code has been developed. The following conclusions can be deduced from this study:

- We can obtain relations of the perfect gas from relations of the model *HT* by canceling all the interpolation constants of the function $C_P(T)$ except the first one. In

this case, the *PG* model becomes a special case of our *HT* model.

- The developed numerical program gives results for any gas found in nature. It is necessary to add $C_P(T)$ and R of the gas and calculate $H(T)$. The application is only made for air.
- The *PG* model gives better results when $M_E<2.00$ and $T_0<1000$ K. It disrupts the performance when M_E and T_0 increase, where the calculation requires the use of our *HT* model for correction.
- The function $C_P(T)$ mainly influence on all the design and the parameters of the plug nozzle.
- The convergence of the results requires an additional calculation time for our *HT* model compared to the *PG* model for the same accuracy.
- If the error is lower than 5%, the result is accepted, so we can study a supersonic flow by using the *PG* relations, if the stagnation temperature is lower than 1000 K for any value of the Mach number, or when the Mach number is lower than 2.00 for any stagnation temperature up to approximately 3500 K.
- For different stagnations temperature T_0, the error between the *HT* and the *PG* models is calculated for different parameters (length, thrust coefficient and mass coefficient). This error increases with the increase of this temperature.
- In terms of design parameters (length, thrust coefficient and mass coefficient), the performances obtained for the axisymmetric nozzle are clearly better than those obtained for bi-dimensional nozzle.
- An extension can be made to determine the physical parameters of the design of a plugging nozzle at high temperature of an arbitrary 3D section by applying the stream-lines method in space [19], for example applications for square or rectangular shapes.

REFERENCES

[1] Sutton G.P, Biblarz O, Rocket Propulsion Elements, Seventh edition, John Wiley & Sons, New York, 2001.

[2] Angelino G, Approximate Method for Plug Nozzle Design, AIAA J., Vol.2, No.10, 1964.

[3] Chang-Hui Wang, Yu Liu, Li-Zi Qin, Aerospike Nozzle Contour Design and Its Performance Validation, Acta Astronautica, Vol 64, pp. 1264-1275, 2009.

[4] Berman K, Performance of Plug-Type Rocket Exhaust Nozzles, ARS Journal, 31(1), 18-23, 1961.

[5] Hagemann G, Immich H, Terhardt M, Flow Phenomena in Advanced Rocket Nozzles the Plug Nozzle, 34th AIAA/ASME/SAE/ASEE Joint Propulsion Conférence and Exhibit, 3522, 1998.

[6] Hagmann G, Immich H, Dumnov G, Critical Assessment of the Linear Plug Nozzle Concept, 37th Joint Propulsion Conférence and exhibit, 3683, 2001.

[7] You-Hong Liu, Experimental and Numerical Investigation of circularly lobed nozzle with/without central plug, International Journal of Heat and Mass Transfer, Volume 45, Issue12, pp. 2577-2585, 2002.

[8] Chang-hui WANG, Yu Liu, Yen-Fei LIAO, Studies on Aerodynamic Behavior and Performance of Aerospike Nozzles . Chinese Journal of Aeronautics, Volume 19, Issue 1, pp. 1-9, 2006.

[9] Miaosheng He, Lizi Qin, Yu Liu, Numerical investigation of flow separation behaviour in an over-expanded annular conical aerospike nozzle. Chinese Journal of Aeronautics, Volume 28, Issue 4, pp. 983-1002, 2015.

[10] Zebbiche T, Youbi Z. Effect of stagnation temperature on supersonic flow parameters application for air in nozzles. Aeronaut J, 16(2), pp. 53–62, 2007.

[11] Zebbiche T, Youbi Z. Supersonic flow parameters at high temperature: application for air in nozzles. In: German aerospace congress, 2005 Sep 26–29; Friendrichshafen, Germany; 2005. pp. 1059 253–65.

[12] Zebbiche, T. Stagnation temperature effect on the Prandtl Meyer function. AIAA J. 45 (4), 952–954, 2007.

[13] Boun-jad M., Zebbiche T. And Allali A., "High temperature gas effect on the Prandtl-Meyer function with application for supersonic nozzle design," Mechanics & Industry, Vol.18, N° 2, 2017.

[14] Zebbiche T. and Youbi Z., "Effect of Stagnation temperature on the Supersonic Two-Dimensional Plug Nozzle Conception. Application for Air," Chinese Journal of Aeronautics 20(1), 15-28, 2007.

[15] Takashi I., Fujii K. and Hayashi A. K., "Computations of Axisymmetric Plug-Nozzle Flow fields: Flow Structures and Thrust Performance," AIAA Journal of Propulsion and Power, Vol. 18, N° 2, pp. 254-260, 2002.

[16] Takashi I. and Fujii K., "Numerical Investigations of the Base-Flow Characteristics of Axisymmetric Aerospike Nozzles," Transations of the Japon Society for Aeronautical and space Sciences, Vol. 45, N° 148, pp. 108-115, 2002.

[17] Anderson, Jr., 1988. Fundamentals of Aerodynamics, 2nd ed., Mc Graw-Hill Book Company, New York.

[18] Démidovitch, B. et Maron I., 1987. Eléments de calcul numérique, Editions MIR, Moscou.

[19] Abada O, Zebbiche T, Abdallah Elhirtsi A, " Three-dimensional supersonic minimum length nozzle design at high temperature for arbitrary exit cross section", Arabian Journal for Science and Engineering, Vol. 39(11), pp. 8233-8245, 2014.

[20] Zebbiche T, "Stagnation temperature effect on the supersonic axisymmetric minimum length nozzle design with application for Air," Advances in Space Research 48, 1658-1675, 2011.